Proposed experiments to grow nanoscale *p-n* junctions and modulation-doped quantum wires and dots

V. Narayan and M. Willander
Physical Electronics and Photonics, Department of Physics, Fysikgränd 3, University of Göteborg, Göteborg, Sweden and Chalmers University of Technology, S-412 96 Göteborg, Sweden
(Received 9 October 2001; published 14 March 2002)

We propose and model several experiments where the field effect defined by split gates is used to restrict acceptors and donors to regions of a semiconductor layer. The nonlinear potential defined by split gates restricts positive donors to the center of the layer, whereas the negative acceptors localize near the edges. The Arrhenius equation modified to include effects of the external and internal fields is used to calculate time- and position-dependent impurity hopping probabilities for Monte Carlo simulations of the experiments. The results show that at high doping levels, the internal field resists high concentrations of net charge, and ''flattens'' the doping profile. In addition, we perform Monte Carlo simulations, where the split gates move relative to the semiconductor sample, to demonstrate how regions of a semiconductor layer can be cleared of unwanted impurities. Finally, we discuss how a ''chessboard'' arrangement of square gates can be employed to create modulation-doped quantum dot arrays.

DOI: 10.1103/PhysRevB.65.125330 PACS number(s): 66.30.Jt, 61.72.Tt

I. INTRODUCTION

The electronic and optical properties of modulation doped semiconductor heterostructures,[1] quantum wires,[2] and quantum dots[3,4] has attracted a great deal of interest, both theoretically and experimentally. These structures all have regions that are selectively doped, a common feature shared with conventional devices such as *p-n* (Ref. 5) diodes and heterojunction bipolar transistors (HBT's).[6,7] Typical structures are grown using a combination of molecular-beam epitaxy (MBE), ion implantation, and selective masking of areas, to create *n*- and *p*-doped regions.[8] The contamination of areas by unwanted impurities can occur, subsequently degrading device performance. It is well known that the impurities ionize at high temperature, then randomly diffuse through the crystal. These charged particles may be accelerated by an external potential[9–11] (usually linear), allowing a measure of control of the doping profile. A recent promising paper demonstrates that an electrically conducting scanning probe microscopy tip can be used to fabricate *nm* scale *p-n-p* junctions.[12] Recently, we have proposed an experiment and performed supporting Monte Carlo simulations where doping profiles in semiconductor layers are controlled by a nonlinear potential defined by split gates.[13]

The split gates defined an approximately harmonic potential,[14] accelerating the impurities to the potential minima. Our model includes both the internal and external fields, and can predict the equilibrium and nonequilibrium impurity profiles as a function of temperature, external voltage, and initial doping profile. The imhomogenous distribution of impurities gives rise to an internal field that will cause considerable broadening of the doping profile[15] at high doping levels. In this paper, we apply the model for a semiconductor layer containing both donors and acceptors. These oppositely charged particles shall be accelerated in opposite directions by the external field, hence a natural separation of particles occurs resulting in the creation of *p-n* junctions. The ''sharpness'' of the doping profile shall be limited by the internal potential, which in turn depends on the impurity concentration gradient.

In addition, we consider an experiment where the split gates can be moved relative to the semiconductor sample, during heat treatment. The external voltage will sweep away unwanted impurities from regions of the semiconductor. We aim to demonstrate the concept rather than carry out an exhaustive study, which is best performed in parallel with future experiments. The split gates which can be moved may perhaps be constructed by borrowing and modifying standard scanning tunneling microscopy (STM) (Refs. 16 and 17) technology. The time dependence of the external potential can be easily incorporated into the Monte Carlo simulation. In comparison, a numerical solution of the drift-diffusion equation coupled to the Poisson equation,[18,19] with an external field that is time dependent, would be difficult, perhaps impossible. Finally, we discuss how low dimensional *p-n* junctions and modulation doped quantum wires and dots maybe fabricated by using a correct configuration of gates.

II. PROPOSED EXPERIMENTS

The cross section of the experimental setup is schematically shown in Fig. 1. The structure is infinitely long in the *z* direction. The semiconductor-oxide interfaces define a central semiconductor layer of length of 70 nm in the *y* direction and width of 30 nm in the *x* direction. The split gates can be mechanically moved, their mutual separation *d* and their distance *h* from the semiconductor sample may be varied. The gates are kept at a fixed voltage v_g and the resulting field effect defines an approximately parabolic potential. In a proposed experiment, the central semiconductor layer has an equal concentration of donors and acceptors. The sample is heated and the impurities ionize, and are accelerated by the external potential. The impurities are assumed to be reflected at the interfaces with the oxide, as the oxide is doped with diffusion inhibiting elements such as nitrogen. The oxide is

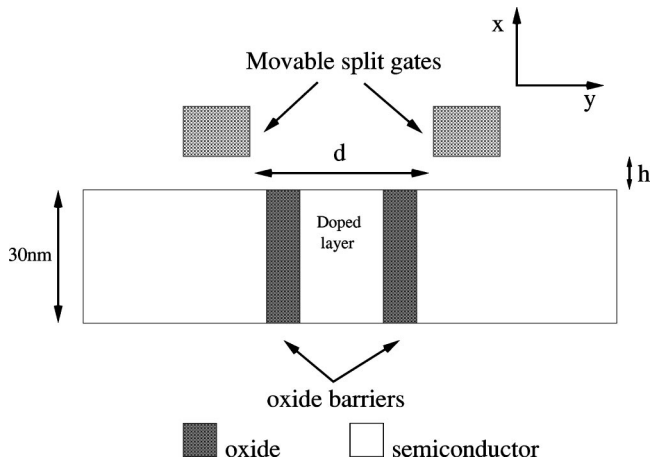

FIG. 1. The diagram of a proposed experiment, not shown to scale. The cross section in the x-y plane is shown of a structure that extends to infinity in the z direction. A doped semiconductor layer is between oxide layers. The metal split gates are movable similar to a scanning tunneling microscope tip. The field effect produced by the gates defines a potential that has an approximate parabolic form in the y direction and is shown to be centered in the middle of the semiconductor layer. The separation between the split gates, the distance from the sample, and the gate voltage can be varied to tailor the curvature of the parabola.

assumed to be polycrystalline, hence diffusion through the oxide would be much slower than diffusion in a near perfect crystal.

The experimental setup for the second proposed experiment contains no oxide layers, only a continuous semiconductor layer. The semiconductor layer is initially evenly n or p doped. The sample is heated and the impurities randomly diffuse in the layer. The split gates are switched on and then from left to right, sweeping impurities in the direction of the split gate motion. We only consider movement in the y direction. The external potential V_{ext} (assuming the gates move at constant velocity in the y direction) is now time dependent and has a parabolic form between the gates,

$$V_{ext}(y,t)=(y-ct)^2, \tag{1}$$

where t is the time and c is a velocity constant. The potential would be constant for the region under the gates (but not too close to the edge of the gate). One would expect that the potential around the edges of the split gates will smoothly fit the parabolic potential and the constant potential regions. The aim of the experiment is to clear impurities from the left region of the semiconductor layer.

III. IMPURITY DIFFUSION WITH A TIME AND POSITION DEPENDENT POTENTIAL

We employ the same Monte Carlo simulation procedure previously used to model the diffusion of a single species of impurity in a semiconductor layer.[13] The method converges rapidly when increasing the number of particles, and shall be easily generalized to include both donors and acceptors. The impurities hop from site to site in the semiconductor lattice. The hopping probability between neighboring sites can be obtained by modifying the Arrhenius equation to include the potential difference between different sites, thus the hopping probability W_{ij} between neighboring sites i and j is given by

$$W_{ij}=D_0\exp\left(\frac{-E_a-V_{ij}/2}{k_BT}\right)dt, \tag{2}$$

where E_a the activation energy, D_0 is the diffusion constant, and V_{ij} is the total potential difference between lattice sites i and j. The activation energies and diffusion constants can be fitted empirically,[8] or estimated by first-principles density-function theory calculations.[20,21] The potential difference V_{ij} is the sum of the external field V_{ext} produced by the split gates and the internal field V_{int} manifesting from a nonhomogeneous distribution of impurities. An effective temperature-dependent time $d\tau=D_0\exp(-E_a/k_BT)dt$ is introduced to express the above equation in the simpler form,

$$W_{ij}=D_0\exp\left(\frac{V_{ij}}{2k_BT}\right)d\tau, \tag{3}$$

where the hopping probability is a function of position in the y direction.

The internal potential shall be calculated by ignoring the discrete nature of the impurities, to allow a simple numerical solution of the Poisson equation,

$$\nabla^2V_{int}(y)=-\frac{\rho_d(y)-\rho_a(y)}{\epsilon}, \tag{4}$$

where $\rho_d(y)$ and $\rho_a(y)$ are the donor and acceptor charge densities, and ϵ is the static dielectric constant of the material. We impose the boundary conditions that $V_{int}=0$ and $\rho(y)=0$ for $y\rightarrow\pm\infty$. We ignore the boundary effects in the x direction, the charge density is assumed to only vary with the y direction.

The electronic charge has been evenly smeared out to ensure charge neutrality of the system, allowing a physical treatment of the Poisson equation. The Debye length at typical growth temperatures and carrier densities is much larger than the intersite distance.[8] The electric field resulting from inhomogeneities in the electron/hole density shall be small for distances much less than the Debye length, and shall be neglected.[15]

The Monte Carlo simulation has the following steps. A constant distribution of impurities are placed at each site (5000 per site in the present study) of a one-dimensional (1D) lattice (each site represents a 2D plane of lattice sites). The internal potential is evaluated to determine the left and right hopping probabilities for each site. A set of random numbers is generated and the impurities are moved. The process is repeated until the impurity density profile has reached equilibrium. The simulation takes roughly 15 min for a lattice with 141 sites on a Sun Ultra 5 machine.

The Monte Carlo approach has been previously used to study the role of the Coulomb repulsion between ionized impurities in effecting doping profiles.[22,15] The simulation approach used in this paper is also reminiscent of a Monte Carlo model on the influence of the local electric field on ionic transport during redox switching of conducting

polymers.[23] The Monte Carlo method described is equivalent to numerically solving coupled drift-diffusion equations (one for each species of impurity) coupled to the Poisson equation.[24] The Monte Carlo approach will converge to the numerical solution as the number of particles approaches infinity and the time step approaches zero.[25] An analytic solution of the problem is only possible for the simplest case, where the internal and external potentials are set to zero,[26] and the Monte Carlo method has been shown to be equivalent to the analytic solution.[27]

We have chosen the Monte Carlo method for its ease of flexibility. A time-dependent external potential representing a moving gate is easily incorporated into the simulation, whereas in a numerical scheme it would not be so trivial. Furthermore, the Monte Carlo approach we believe is simple to implement when modeling real experiments. During device processing, there are usually several steps, each for separate lengths of time and temperature. The Monte Carlo simulation carefully used can be easily modified to simulate the time-dependent temperature. In addition, the Monte Carlo approach is most appropriate for considering controlled diffusion to fabricate quantum dots, since the system will contain a finite number of impurities, which for a low doping level can be a relatively small number. The Monte Carlo method can also be easily modified to consider a layered system where the diffusion constant is material dependent.

IV. NUMERICAL RESULTS

The results are presented for a 1D lattice with 141 sites and the separation between sites is fixed to 0.5431 nm. The dielectric constant $\epsilon = 11.4$ which is the value for silicon. The parameters are set as follows: unit time $\tau = 0.37$ and temperature $T = 600$ K, to allow a significant probability of impurity hopping per unit time. The value of unit time is arbitrary as we are interested in the general time dependence of the diffusion. The donors and acceptors have been set to have equal diffusion constants and Arrhenius activation energies. However, these parameters can be easily changed. The form of the external potential is shown in Fig. 2 which has a parabolic form for the sites labeled between -50 and 50. The maximum value of the potential in this region is defined as $V_{ext}(P)$. The potential for sites between ± 70 to ± 55 is fixed to a constant value of $1.1V_{ext}(P)$. Then cubic spline is performed, to smoothly fit the parabolic potential and the constant potential regions. The constant potential regions are directly under the split gates, whereas the parabolic potential is located in the gap region between the gates. The connecting region represents the potential around the edges of the split gates.

Figures 3(a) and (b) show the distribution of donors and acceptors after 1000 units of time, for $V_{ext}(P)$ between 2.0 and 0.3 eV, where the initial doping level has been set to 10^{17} cm^{-3}. The sign of the external potential is chosen so that the positive charges of the donors are accelerated to the center and the acceptors migrate to the edges. A clear separation of the positive and negative charges has occurred, an *n-p-n* structure has been created. These doping profiles have been compared with a simulation that neglects the internal potential. We infer for this doping level that the internal field is very weak, and the impurity migration is dominated by the external potential. The external field accelerates acceptors from the central region to sites ± 55, whereas acceptors in the constant potential regions are reflected at the interfaces with the oxide and perform a random walk, with equal probability of hopping left or right, the net result being that the acceptor concentration peaks at sites ± 55. We note a region with a very low concentration of impurities. Evidently, the width of this region, including the ''sharpness'' of the donor and acceptor regions, can be controlled by the curvature of the external potential.

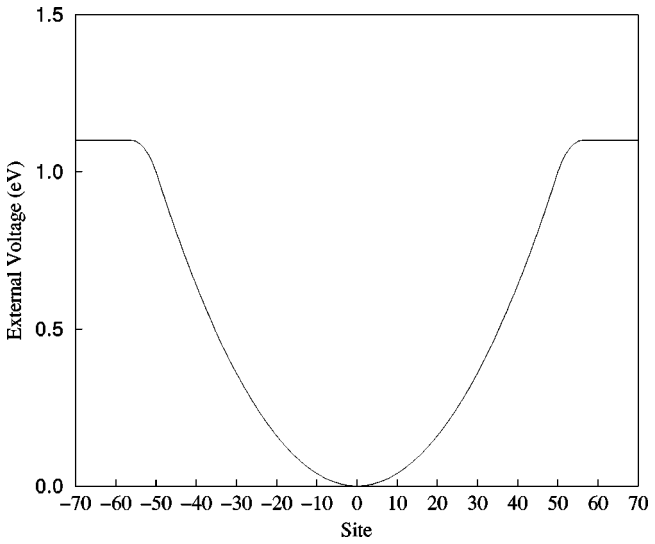

FIG. 2. The form of the external potential. The region of constant potential is directly below the gates, whereas the parabolic region is located at the gap between the gates. These regions are fitted using cubic spline.

Figures 4(a) and (b) show the distribution of donors and acceptors, after 1000 units of time, for $V_{ext}(P)$ between 2.0 and 0.3 eV, where the initial doping level has been set to 10^{18} cm^{-3}. The donor distributions have been broadened by the internal potential which is relatively strong. The internal field builds up at the middle when donors flood the center and resists further net migration of donors. The internal field also resists buildup of acceptors at the edges, accelerating acceptors to sites ± 55. However, there is a limit to how much charge can be built up around sites ± 55, since this is also resisted by the internal field. We note that the acceptor distribution has become sharper for this doping level, and we attribute this feature to being caused by a stronger internal field. The donor distributions, however, are much broader and a stronger external field is required to separate the negative and positive charges.

Figures 5(a) and (b) show the distribution of donors and acceptors for an initial doping density 10^{19} cm^{-3}. The internal field is extremely strong at this doping level and the donor distributions are nearly constant except near the edges. The acceptors are also evenly distributed, but still peak around sites ± 55, though the peaks are low in comparison to distributions presented for the other lower doping levels. The

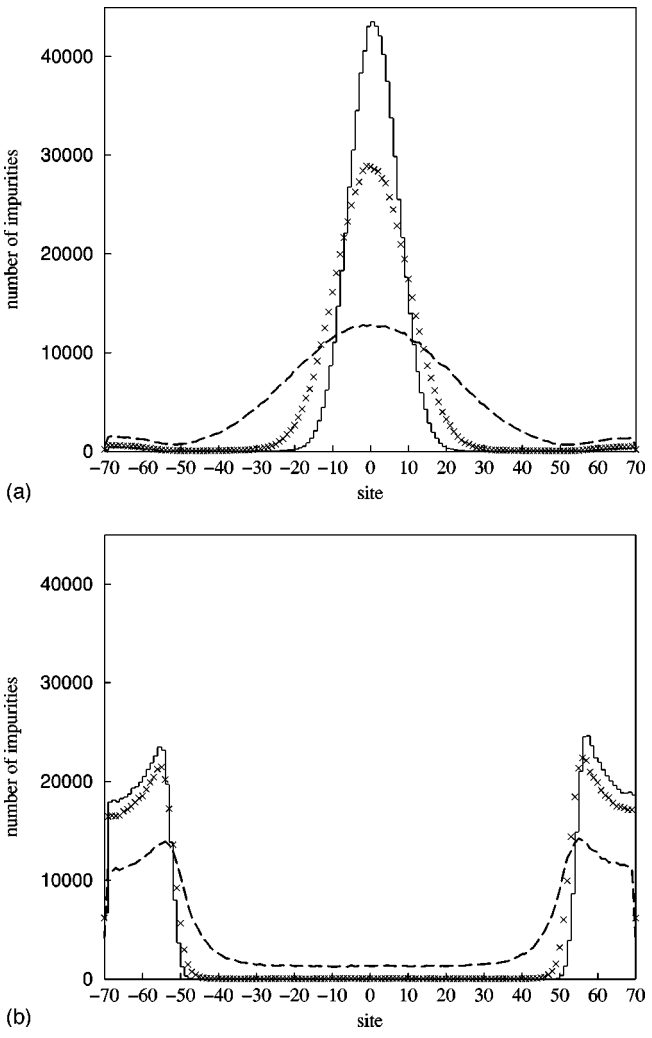

FIG. 3. The graph of the number of (a) positive and (b) negative impurities at each site after 1000 time steps. The external potential $V_{ext}(P)$ imposed by the split gates has the values 2.0 eV (solid lines), 1.0 eV (crosses), and 0.3 eV (dashed line), respectively. The doping density at the start of the simulation is set to 10^{17} cm^{-3}.

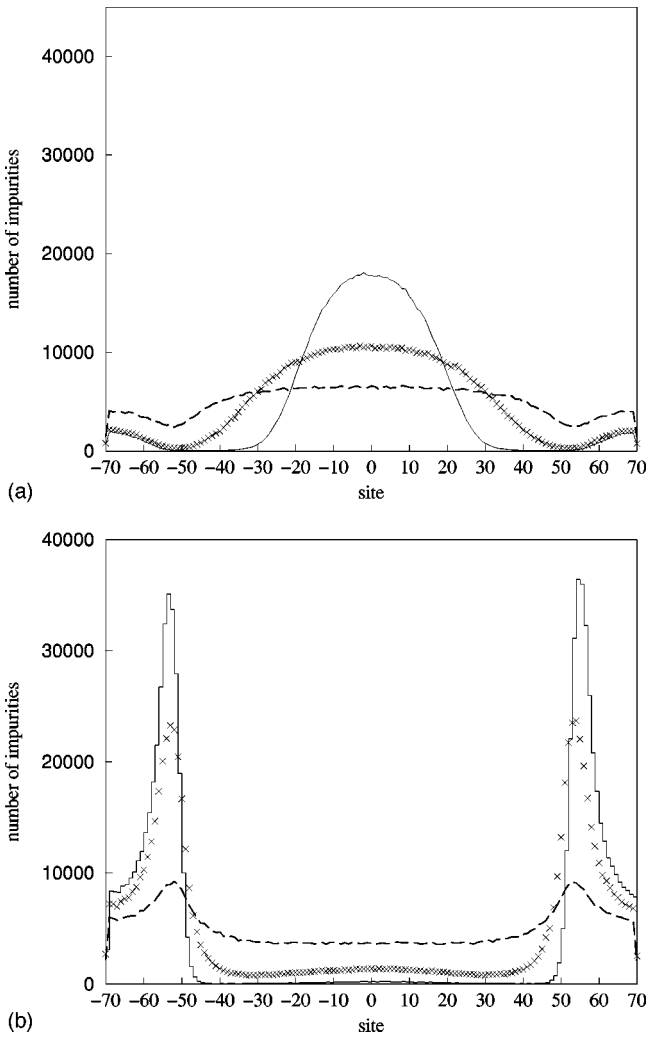

FIG. 4. The graph of the number of (a) positive and (b) negative impurities at each site after 1000 time steps. The external potential $V_{ext}(P)$ imposed by the split gates has the values 2.0 eV (solid lines), 1.0 eV (crosses), and 0.3 eV (dashed line), respectively. The doping density at the start of the simulation is set to 10^{18} cm^{-3}.

external field has failed to separate the positive and negative charge, and no clear p-n junctions have been created.

The modeling of real experiments would require an accurate modeling of the split gates, which should be done in conjunction with real experiments. The height of the peaks in the acceptor concentration depends on the form of the potential in the region at the edges of the split gates, and the width of the regions of constant potential. We are confident that our model describes the trends of the real physical system. Further experiments may be performed where a series of split gates are used to create a series of quantum wire p-n junction and modulation-doped quantum wire arrays.

We finally consider Monte Carlo simulations where the split gates are moved from left to right in the y direction. The lattice in the simulation consists of 1001 sites. The first 141 sites are defined as in Fig. 2. During the simulation the region shown in Fig. 2 is moved at a rate of one site per unit time, from left to right. The potential at the remaining sites is fixed to 1.1 eV. The simulation is run for 1000 units of time and the split gates only move for the first 9860 time steps so that the potential shown in Fig. 2 has been displaced to the right edge of the sample. Figure 6 shows the impurity distribution after 1000 units of time for initial doping levels fixed to 10^{18} and 10^{19} cm^{-3}, respectively. The impurity distribution peaks at the final position of the parabolic region. However, a constant density of impurities remains throughout the sample. The gates should be moved more slowly to trap more particles in the parabola. The clearing of impurities would be effective for low impurity levels and low gate velocity.

V. FABRICATING ARRAYS OF QUANTUM DOTS

The ideas presented can be generalized to fabricate an array of quantum dots. A chessboard arrangement of gates shown in Fig. 7 may be fabricated on top of an oxide layer that protects a doped semiconductor layer resting on an oxide substrate. We assume the impurities diffuse much faster in

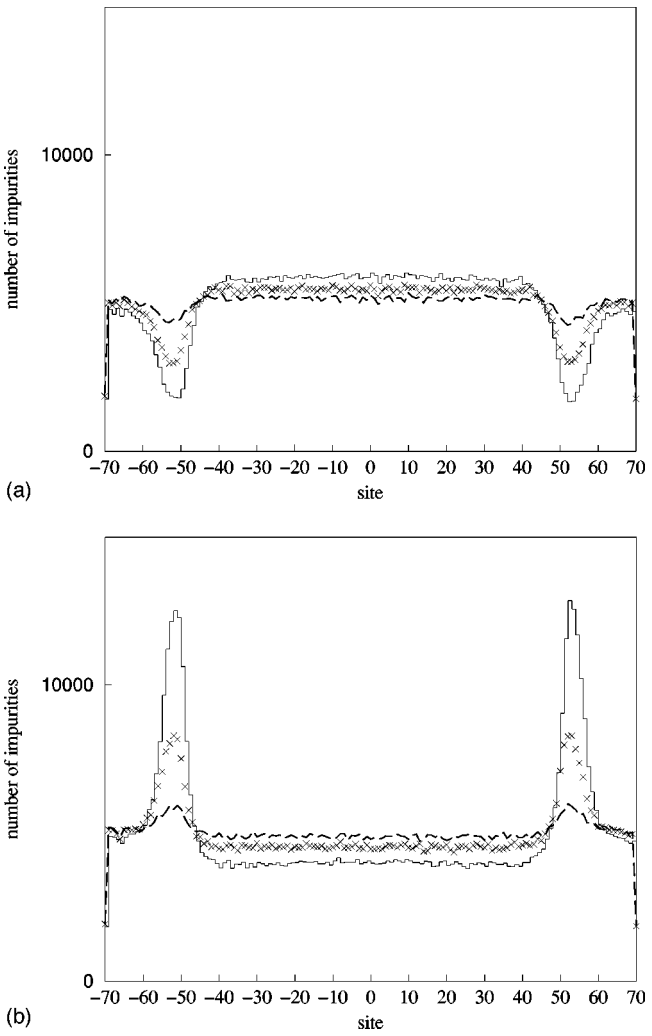

FIG. 5. The graph of the number of (a) positive and (b) negative impurities at each site after 1000 time steps. The external potential $V_{ext}(P)$ imposed by the split gates has the values 2.0 eV (solid lines), 1.0 eV (crosses), and 0.3 eV (dashed line), respectively. The doping density at the start of the simulation is set to 10^{19} cm^{-3}.

the semiconductor than the oxide layers. Ideally, one would like to replace the oxide layer by a material which cannot be penetrated by the impurities. The square gates will define a potential that is approximately harmonic in the x and y directions.[28] During heat treatment the donors will migrate to a line in the z direction which passes through the center of the gates, whereas the acceptors would migrate away from the gates, thus quantum dot p-n junctions are formed. Modulation-doped quantum dot arrays can be created only if donors or acceptors are present in the semiconductor layer.

The short-range impurity-impurity interaction[15] would most likely be very important for such a system particularly at high doping levels, and our model would need considerable refinement. Furthermore, during the processing of quantum dots which have sizes of the order of the bulk Debye screening length, the approximation of evenly smearing out the electronic charge would not be physical. Therefore the quantum mechanics of the electronics states should be considered, as well as many-body effects. The gates should be

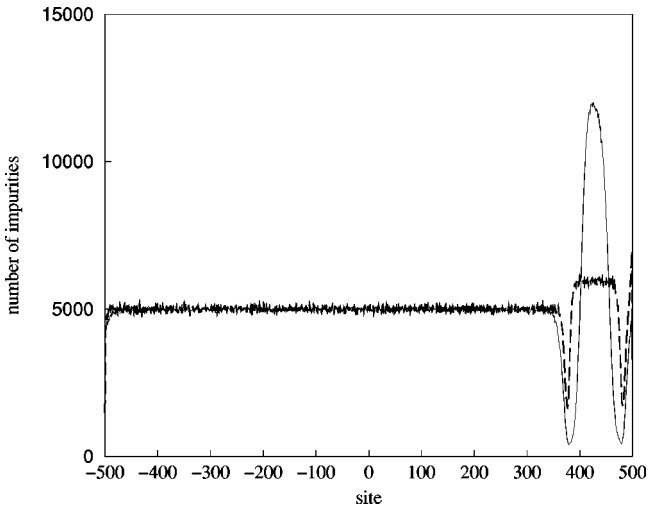

FIG. 6. The graph of the number of positive impurities at each site after 1000 time steps. The initial doping density was set to 10^{19} cm^{-3} (dotted line) and 10^{18} cm^{-3} (solid line). The lattice contains 1000 sites. The external potential has a maximum value of 1.1 eV.

identical to ensure that nearly identical dots are formed. We note that using self-assembled techniques,[29] quantum dots are formed at random sites with a statistical distribution of sizes. In contrast, our proposed method can in principle produce dots at selected positions and sizes. The quantum arrays could be used as quantum dot lasers and photodetectors. In addition, more intricate arrays of gates can be employed to customize the quantum dot arrays.

VI. SUMMARY AND DISCUSSION

Experiments have been proposed to achieve controlled impurity diffusion of donors and acceptors on the nanometer

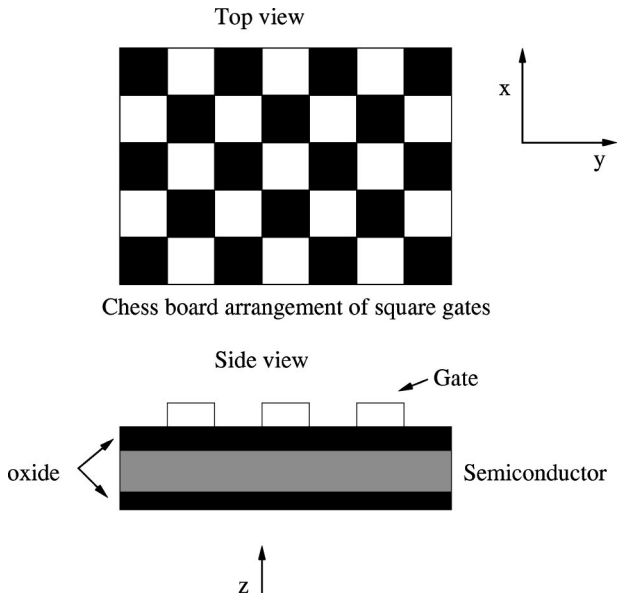

FIG. 7. The diagram shows a chessboard arrangement of square gates. The gates are placed on an oxide layer that is grown on a n-doped semiconductor layer resting on an oxide substrate.

scale to fabricate nanometer scale *p-n* junctions. The simulations show that a charge segregation fails at high doping levels, which is in agreement with experiment and supporting simulations that show that the Coulomb interaction imposes a maximum concentration of impurities in a semiconductor.[22] In addition, a model has been proposed which is simple but we believe accurately describes the physical trends of the system. The Monte Carlo simulations indicate that nanometer scale *p-n-p* or *n-p-n* junctions maybe fabricated and the doping profile can be controlled. The doping profile will depend on the split gate voltages, the diffusion constants, and Arrhenius activation energies. The model has also been generalized to included a time-dependent external field. Monte Carlo simulations were performed where the gates move relative to the semiconductor sample. Using this setup, areas contaminated by impurities may be cleaned. Finally, experiments where proposed where arrays of near identical quantum dots can be formed.

The model described only treats the internal field in a mean-field sense, this would most likely be accurate for low and moderate doping levels. At high doping levels, however, the true internal potential can produce large random potentials in the vicinity of a given impurity caused by short range impurity interactions. The random potentials have a greater chance of occurring with increasing doping density, which may cause broadening of δ-doped layers after a critical doping density.[15] The technology exists at present, where most of the described experiments can be tried. However, movable split gates have not yet been created. We hope this paper will inspire experimental work and complementary theoretical analysis.

ACKNOWLEDGMENTS

This work was funded by a TMR network (contract number ERB4061PL95) of the fifth framework program of the European Union. V. Narayan would like to thank M. Yousif, I. Choquet, J. K. Vincent, and P. Sunqvist for useful and stimulating discussions.

[1] G. D. Sanders and Y. C. Chang, Phys. Rev. B **31**, 6892 (1985).
[2] F. A. Reboredo and C. R. Proetto, Phys. Rev. B **50**, 15 174 (1994).
[3] G. Gumbs, D. Huang, H. Qiang, F. H. Pollak, P. D. Wang, C. M. S. Torres, and M. C. Holland, Phys. Rev. B **50**, 10 962 (1994).
[4] T. Inoshita, S. Ohnishi, and A. Oshiyama, Phys. Rev. B **38**, 3733 (1998).
[5] W. Shockley, Bell Syst. Tech. J. **28**, 435 (1949).
[6] K. P. Clark, W. P. Kirk, and A. C. Seabaugh, Phys. Rev. B **55**, 7068 (1997).
[7] M. J. Kelly, *Low-Dimensional Semiconductors* (Oxford University, New York, 1995).
[8] E. F. Schubert, *Doping in III/V Semiconductors* (Cambridge University Press, Cambridge, England, 1993).
[9] E. M. Pell, J. Appl. Phys. **31**, 291 (1954).
[10] G. Popovici, T. Sung, S. Khasawinah, M. A. Prelas, and R. G. Wilson, J. Appl. Phys. **77**, 5625 (1995).
[11] T. Sung, G. Popovici, M. A. Prelas, R. G. Wilson, and S. K. Loyalka, J. Mater. Res. **12**, 1169 (1997).
[12] S. Richter, Y. Manassen, and D. Cahen, Phys. Rev. B **59**, 10 877 (1999).
[13] V. Narayan and M. Willander, Phys. Rev. B **65**, 075308 (2002).
[14] Y. Sun, G. Kirczenow, A. S. Sachrajda, and Y. Feng, J. Appl. Phys. **77**, 6361 (1995).
[15] N. S. Averkiev, A. M. Monakhov, A. Shik, P. M. Koenraad, and J. H. Wolter, Phys. Rev. B **61**, 3033 (2000).
[16] J. Tersoff and D. R. Hamann, Phys. Rev. B **31**, 805 (1985).
[17] H. H. Farrell and M. Levinson, Phys. Rev. B **31**, 3593 (1985).
[18] A. Arnold, P. Markowich, and G. Toscani, Transp. Theory Stat. Phys. **29**, 571 (2000).
[19] A. A. Moya, A. Hayas, and J. Horno, Solid State Ionics **2**, 9 (2000).
[20] M. Hakala, M. J. Puska, and R. M. Nieminen, Phys. Rev. B **61**, 8155 (2000).
[21] P. Alippi, L. Colombo, and P. Ruggerone, Phys. Rev. B **64**, 075207 (2001).
[22] E. F. Schubert, G. H. Gilmer, R. F. Kopf, and H. S. Luftman, Phys. Rev. B **46**, 15 078 (2001).
[23] F. Miomandre, M. N. Bussac, E. Vieil, and L. Zuppiroli, Chem. Phys. **255**, 291 (2000).
[24] I. Rubinstein and L. Rubinstein, *Partial Differential Equation in Classical Mathematical Physics* (Cambridge University Press, Cambridge, England, 1993).
[25] I. Coulibaly and C. Lecot, Math. Comput. Simul. **47**, 153 (1998).
[26] P. M. Fahey, P. B. Griffin, and J. D. Plummer, Rev. Mod. Phys. **61**, 289 (1989).
[27] V. Narayan, BS dissertation, Department of Physics, University of East Anglia, Norwich, England, 1991.
[28] A. Kumar, S. E. Laux, and F. Stern, Phys. Rev. B **42**, 5166 (1990).
[29] L. Veskan, M. Goryll, T. Stoica, P. Gartner, K. Grimm, O. Cretien, E. Mateeva, C. Dieker, and B. Hollander, Appl. Phys. A: Mater. Sci. Process. **71**, 423 (2000).